THE JOURNAL OF PHYSICAL CHEMISTRY A

Article

pubs.acs.org/JPCA

Ferric–Thiolate Bond Dissociation Studied with Electronic Structure Calculations

Guilherme Menegon Arantes*,† and Martin J. Field‡

†Department of Biochemistry, Instituto de Química, Universidade de São Paulo, Av. Prof. Lineu Prestes 748, 05508-900, São Paulo, SP Brazil

‡Institut de Biologie Structurale (IBS), CEA/CNRS/Université Joseph Fourier, 71 Avenue des Martyrs, CS 10090, 38044 Grenoble Cedex 9, France

Supporting Information

ABSTRACT: The stability and reactivity of iron–sulfur clusters are fundamental properties for the biological function of these prosthetic groups. Here, we investigate the ferric–thiolate bond dissociation of model iron–sulfur tetrahedral complexes with high-level ab initio multiconfigurational electronic structure calculations. We find that the reaction mechanism is homolytic with a spin-crossing from the sextet state in the reactant to quartet state in the product. We also compare several density functionals and semiempirical configuration interaction with the high-level ab initio results to find an accurate but computationally more efficient method to describe the reaction. The functionals M06 and those based on the OPTX exchange functional show the best performance and may reasonably describe the various electron correlation effects involved in ferric–thiolate bond dissociation.

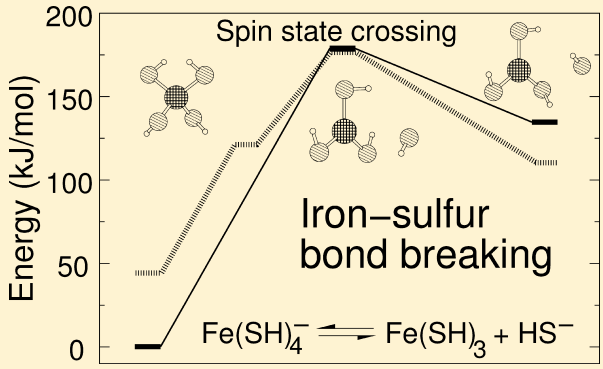

1. INTRODUCTION

Iron under various oxidation states is commonly found in biomolecules tetrahedrally coordinated to thiolate or inorganic sulfide ligands. These iron–sulfur clusters are involved in many complex and essential biochemical processes that depend on redox reactions,[1−3] such as photosynthesis, cellular respiration, and signaling.

Recently,[4−6] atomic force microscopy (AFM) and molecular modeling with quantum chemical calculations were used together to probe the stability and reactivity of ferric–thiolate bonds in a simple iron–sulfur protein, rubredoxin. This protein contains one iron center coordinated by the side-chains of four cysteines.[7] Our aims in the study presented here are to investigate the intrinsic properties of ferric–thiolate bond dissociation, free from protein or solvent interactions, and to find a good balance between accuracy and efficiency in its description by comparing several different electronic structure methods.

Modeling ferric–thiolate dissociation by quantum chemical methods is a difficult problem. The multiplet structure of iron (d^5 in the ferric redox state) and its spin manifold, as well as the bond-breaking process, result in near-degenerate electronic configurations that should, in principle, be described by multiconfigurational methods.[8] One approach that has been able to correctly describe near-degenerate effects in transition-metal compounds is the complete active space (CAS) self-consistent field (SCF) method,[9] especially when some dynamic electron correlation is also perturbatively recovered, as in its CASPT2[10] variant. This method has been successfully applied in a number of studies of iron complexes.[11−14]

Density functional theory (DFT)[15] has been used extensively to calculate the electronic structure of transition-metal compounds.[16] Given the approximate nature of the available exchange-correlation functionals it is not evident whether the aforementioned electron correlation effects, nondynamic from near-degeneracies and dynamic from Coulomb interactions, are included in a balanced way. As a result, the performance of several functionals has been tested for different iron complexes.[14,16−27]

It was recognized early that the inclusion of Hartree–Fock (HF) exchange into hybrid DFT functionals increases the relative stability of configurations with unpaired electrons.[17] Consequently, the energy splittings between different spin states of iron–sulfur complexes could be tuned by optimizing the amount of exact exchange added in, for example, the B3LYP functional.[17] It was also shown that the addition of exact exchange underestimates metal–ligand bond energies and that pure-GGA (generalized gradient approximation) functionals overestimate them.[19] A comparison of several metal–ligand diatomics and models of metalloprotein active-sites containing iron centers[20] suggested that a good balance could be obtained with the TPSSh functional.[28] Another comparison that included

Received: June 13, 2015
Revised: September 8, 2015
Published: September 9, 2015

DOI: 10.1021/acs.jpca.5b05658
J. Phys. Chem. A 2015, 119, 10084−10090

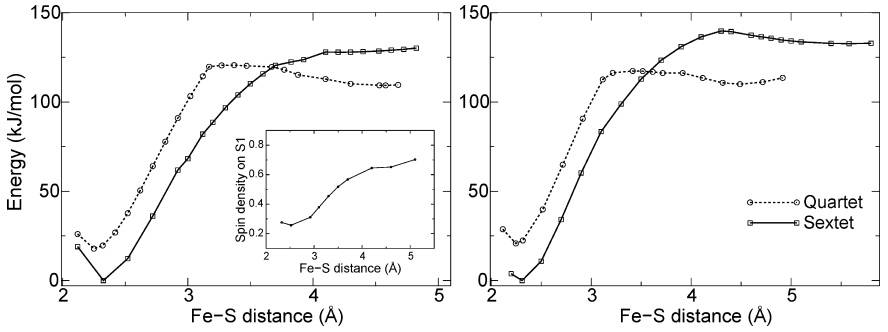

Figure 1. Relative energy profiles for ferric−thiolate bond dissociation obtained at the DFT level. Calculations were carried out at the B3LYP/6-31+G(2df,p) level in the quartet (dashed line) and sextet (solid line) spin states for $Fe(SH)_4^-$ (left panel) and $Fe(SCH_3)_4^-$ (right panel). The inset shows the spin density over the dissociating sulfur atom (S1) for the sextet state.

ferrous and ferric complexes with tetrahedral coordination[14,18] suggested that functionals such as OLYP and OPBE, based on Handy and Cohen's OPTX pure-GGA exchange functional,[29] are the most computationally cost-effective in describing iron compounds.

Here we investigate ferric−thiolate bond dissociation in the following two isolated model reactions

$$Fe(SH)_4^- \rightleftharpoons Fe(SH)_3 + HS^- \quad (1)$$

$$Fe(SCH_3)_4^- \rightleftharpoons Fe(SCH_3)_3 + H_3CS^- \quad (2)$$

using several DFT functionals and multiconfigurational ab initio (CASPT2) and semiempirical[30] methods. Details of the reaction mechanisms, spin states and densities, electronic configurations, and relative energetics are given in the following sections. These results are used to help identify an accurate and efficient treatment of the dissociation reaction.

2. COMPUTATIONAL METHODS

Molecular geometries for species along reactions 1 and 2 were optimized at the DFT level with the B3LYP functional[31,32] and the 6-31+G(2df,p)[33] basis set for all possible electronic spin states (S = 0.5, 1.5, and 2.5). Spin-polarized orbitals were adopted. Optimizations conducted with the TZVP basis set[34] resulted in equivalent structures. Ferric−thiolate bond dissociation was obtained by optimizing the geometry with the dissociative Fe−S distance fixed at a given value. The GAUSSIAN 09 program (rev. A1)[35] was used for geometry optimizations. It should be noted that the calculated Fe−S bond length for the reactant ground state (2.32 Å) is in good agreement with the experimental bond lengths observed in crystallographic structures of proteins that contain tetrahedral Fe−S centers. As an example, in rubredoxin (PDB ID 8RXN), the bond lengths are in the range of 2.27−2.30 Å.

A minimum-energy crossing point (MECP) between sextet and quartet electronic states was optimized with the pDynamo library[36] as described previously[5] with the B3LYP functional and the TZVP basis set.

Single-point DFT energies for geometries corresponding to the CASPT2 low-energy pathway described below were obtained with the ORCA program version 3.0.1[37] and the following functionals: OLYP, O3LYP,[29,32] OPBE,[29,38] PBE0,[39] BLYP,[32,40] B3LYP, B3LYP-D3, BP86,[40,41] TPSS, TPSSh,[28] M06,[42] and B2PLYP.[43] Spin-polarized orbitals and standard integration grids were adopted. The Def2-TZVP basis set[44] and resolution of identity with the TZV/J[45] auxiliary basis were used. A second-order SCF optimization had to be activated to obtain convergence in several cases.

Although the $Fe(SH)_4^-$ ground state (reactant in sextet electronic spin) belongs to the S_4 molecular point group, the tetrahedral symmetry around the iron center is broken in all other geometries studied here. Thus, all calculations were carried out in the C_1 point-group symmetry.

Single-point multiconfigurational calculations were carried out with the geometries optimized by DFT along the ferric−thiolate bond dissociation. The active space was not built using an analysis of the corresponding irreducible representations (irreps) and symmetry adapted linear combinations of ligand molecular orbitals. Instead, it was chosen with five molecular orbitals for the metal 3d open-shell, as these are necessary to describe the near-degenerate configurations arising from the ferric ion multiplet structure, and two extra pairs of correlating molecular orbitals (MOs) describing the bond dissociation process. This active space contained nine electrons in nine orbitals. Similar choices, such as seven electrons in seven MOs, were also tried and yielded equivalent results. The *double-shell* effect[11] was tested for the ferric ion complexes studied here with an active space of nine electrons in fourteen orbitals and found to be negligible (Table S3).

All multiconfigurational CASSCF and CASPT2[8,10] calculations were performed with the MOLCAS program, version 7.4.[46] The ANO-RCC basis-set[47] with contractions Fe-[7s6p5d2f1g], S[6s5p3d2f], and H[3s2p1d] was employed as this was shown to be appropriate in previous benchmark calculations for iron compounds.[12] CASSCF orbitals were optimized for the average of the first three roots with equal weights. Scalar relativistic effects were included using a Douglas−Kroll−Hess Hamiltonian. In all CASPT2 calculations the core electrons were frozen (26 frozen MOs), and only the valence space was correlated. The standard IPEA shift of 0.25 au and an extra denominator shift of 0.3 au were used to avoid intruder states.[10,48]

To test if semiempirical potentials could be used to model ferric−thiolate bond dissociation, the performance of the modern PM6 parametrization[30] that contains d-orbitals in its minimal basis set was investigated with complete active space configuration interaction (CASCI) calculations.[8] Several active spaces were tested for these semiempirical calculations, and the best results were obtained with seven electrons in seven MOs space. Orbitals were determined from restricted-open shell (ROHF) calculations with fractional occupation.[49,50]

The performance of the original PM6 parametrization was very poor (see Results and Discussion); therefore, a specific

DOI: 10.1021/acs.jpca.5b05658
J. Phys. Chem. A 2015, 119, 10084−10090

reparametrization for iron was carried out. CASPT2 energies reported here for Fe−S bond dissociation, iron atomic multiplet and ionization energies taken from spectroscopical data,[51] and DFT energies for different $Fe(SH)_4^-$ and $Fe(SCH_3)_4^-$ geometries (not shown) were used as target or reference properties. Optimized parameters are given in the Supporting Information (Table S1). Full details of the reparametrization procedure are not relevant for the conclusions drawn here and will be given in a future publication. All semiempirical calculations were done with the pDynamo library.[36]

3. RESULTS AND DISCUSSION

3.1. Energy Profiles for Bond Dissociation. Our calculation results for reaction 1 show the ground-state reactant is a sextet spin state and has a tetrahedral geometry belonging to the S_4 point group. The quartet and doublet reactants have distorted tetrahedral coordination around the iron center with overall C_2 symmetry. All other geometries along the Fe−S dissociation belong to the C_1 point group.

The DFT energy profiles shown in Figure 1 for both $Fe(SH)_4^-$ and $Fe(SCH_3)_4^-$ dissociation have several noteworthy features. First, the quartet reactant lies 20 kJ/mol higher in energy than the sextet reactant. However, the lowest-energy product of bond dissociation is a quartet. Thus, there is a spin crossing along the reaction. A minimum-energy crossing point was optimized at a ferric−thiolate bond distance d(Fe−S) ≈ 3.7 Å. Products in all spin states are ion−molecule complexes with small (<4 kJ/mol) recombination barriers. Also, the quartet transition-state region is reached before the MECP, whereas the sextet transition-state region is reached after the MECP. The doublet state energy profile is not shown nor discussed in detail here as all doublet stationary geometries along ferric−thiolate bond dissociation lie at least 90 kJ/mol higher than the other spin states.

The ferric−thiolate bond dissociation mechanism can be deduced from the DFT profiles. Although the reactants have a formally ferric center, both sextet and quartet products have a ferrous center with a dissociated thiolate radical. To illustrate this, the inset in Figure 1 shows that the spin density in the dissociative sulfur atom (S1) changes rather smoothly from 0 to 1 during Fe−S bond dissociation. As a result, Fe−S bond dissociation in both sextet and quartet spin states is homolytic.[5]

The energetics, iron coordination, and Fe−S bond distances of stationary points are very similar between the $Fe(SH)_4^-$ and $Fe(SCH_3)_4^-$ dissociation profiles. Thus, the conclusions drawn below for $Fe(SH)_4^-$ should be equally valid for $Fe(SCH_3)_4^-$ when comparing the different CASPT2, DFT, and semiempirical methods. The only caveat concerns the product region as different d(Fe−S) distances are observed because of the bulkier methyl groups in $Fe(SCH_3)_4^-$ (Figure 1). A related observation should also be made for the products of ferric−thiolate bond cleavage in $Fe(SH)_4^-$ optimized with the OPBE and TPSSh functionals (data not shown). For these two functionals, the products resulted in H_2S instead of HS^-, as this leaving group removes a proton from another thiol group at d(Fe−S) > 4 Å.

The multiconfigurational CASPT2 energy profile for $Fe(SH)_4^-$ dissociation is shown in Figure 2. The energies and structures reported in this figure correspond to the CASPT2 minimum-energy pathway for ferric−thiolate bond dissociation with DFT optimized geometries. These six structures, along with the doublet product and reactant structures (not shown in the figure), will be termed in what follows as reactants (R), transition state (TS), MECP, and products (P), together with their respective total spin electronic state, which can have doublet (^{2}), quartet (^{4}), and sextet (^{6}) multiplicities.

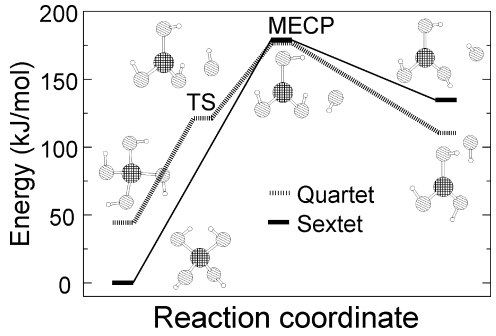

Figure 2. Relative energy profiles for $Fe(SH)_4^-$ ferric−thiolate bond dissociation obtained at the CASPT2 level. Calculations were carried out with the ANO-RCC basis set for the quartet (dashed line) and sextet (solid line) spin states. Structures are shown in ball−stick representation with iron in crossed lines and sulfur in diagonal lines.

The reaction coordinates of the low-energy species along the CASPT2 minimum-energy pathway are similar to those found with DFT. However, we were unable to identify a ^{6}TS with the CASPT2 single-point calculations because of the rather flat transition region observed in the DFT profile [d(Fe−S) > 4 Å in the left panel of Figure 1]. The relative energies for the quartet and sextet profiles found with CASPT2 differ at most by 20 kJ/mol from those obtained with B3LYP for all species except the MECP (Table S2). This is the accuracy (∼20 kJ/mol) often expected of hybrid functionals in isodesmic processes involving metals, such as heterolytic bond dissociations.[19] However, at the crossing point, the difference in relative energy between the B3LYP and CASPT2 energy profiles is higher (50 kJ/mol), which can be partially attributed to a structural relaxation energy not included in our CASPT2 single-point calculations. Although the ^{6}MECP and ^{4}MECP CASPT2 energies differ by less than 4 kJ/mol, indicating that they might be near a surface crossing, the structure still could be far from the true minimum-energy crossing of the CASPT2 energy surfaces. Further comparisons between the multiconfigurational results and several DFT functionals will be given in the next section.

A homolytic reaction mechanism with a spin crossing along the dissociation is also observed in the CASPT2 results. The reactant is in a sextet state, and the most stable product is in the quartet state containing a partial thiolate radical and a ferrous center. However, instead of changing smoothly as in the monoconfigurational DFT calculations (inset in Figure 1), CASSCF spin-densities change abruptly during dissociation as a consequence of hopping between surfaces with different electronic configurations. As shown in Table 1 for the reactant states, almost no spin density is seen on sulfur atoms and the spin density on the iron atom equates to the expected number of unpaired electrons in the spin state. For the MECP, spin densities correspond to different electronic configurations, and spin unpairing is already evident on the dissociating sulfur atom (S1). In fact, the crossing between the sextet and quartet spin states is equivalent to a spin flipping over this sulfur atom. Electronic configurations and, consequently, spin densities are similar between the MECP and product states for both sextet and quartet spin states.

DOI: 10.1021/acs.jpca.5b05658
J. Phys. Chem. A 2015, 119, 10084−10090

Table 1. Mulliken Spin Populations Calculated from the CASSCF Wavefunction for Fe and S Atoms in Structures from Reaction 1[a]

	Fe	S1	S2	S3	S4
^{2}R	1.00	−0.03	0.02	−0.02	0.02
^{2}P	1.34	−0.29	−0.01	−0.00	−0.04
^{4}R	3.11	−0.02	−0.03	−0.03	−0.02
^{4}TS	3.50	−0.50	−0.07	0.03	0.03
^{4}MECP	3.52	−0.52	0.03	0.03	−0.05
^{4}P	3.50	−0.53	0.03	0.03	−0.05
^{6}R	4.75	0.06	0.06	0.06	0.06
^{6}MECP	3.91	0.86	0.03	0.03	0.14
^{6}P	3.91	0.84	0.03	0.18	0.02

[a]The spin density moduli were less than 0.02 for all hydrogen atoms in all structures.

In the calculations for ^{6}R employing spatially restricted orbitals (ROHF and CASSCF), we observe a typical molecular orbital ordering equivalent to what is usually expected from d^5 metal centers with tetrahedral coordination.[52] The valence orbitals of the sulfur ligand combine into nonbonding MOs belonging approximately to the T_1 irrep in the T_d local symmetry around the iron center and into bonding MOs belonging to irreps A_1, E, and T_2. The five unpaired electrons of the metal are distributed in e^2 t_2^3-like orbitals, with contributions of about 5−10% weight from ligand orbitals from irreps E and T_2. For the other geometries along the reaction pathway, the local symmetry around the iron center is distorted and it is more difficult to label the symmetry of the MOs. The ferric−thiolate bond that is broken upon dissociation has a σ character.[3] All the occupied bonding and nonbonding ligand orbitals lie lower in energy than the metal d-shell. This is in contrast to the orbital ordering observed in our DFT unrestricted calculations in which an inverted level-scheme is found due to strong spin polarization of the MOs. The MO ordering in the inverted-level scheme shows the metal d-shell below the ligand bonding and nonbonding MOs. This has also been observed in similar iron−sulfur compounds and extensively discussed by Noodleman et al.,[53−55] Solomon et al.,[56] and more recently by Ichiye and co-workers.[22,57]

Wave functions for all species in the sextet state show a single configuration with more than 98% of the weight in the CI expansion. The other two reactant states, ^{4}R and ^{2}R, are dominated by a single configuration with ≈80% weight in the CI expansion, and the remaining configurations account for different occupations of the metal d-shell. All other quartet and doublet species have large mixtures of configurations without any surpassing 20% weight. These results suggest that monoconfigurational electronic structure methods may be able to describe the bond-breaking process properly in only the sextet state.

3.2. Comparison with DFT Functionals and Semiempirical Methods. To test the performance of more approximate electronic structure methods in the description of ferric−thiolate bond dissociation, we compared the CASPT2 relative energies with a series of DFT functionals and semiempirical methods. Table 2 shows the deviations and maximum errors obtained, and Table S2 in the Supporting Information gives the relative energy values. We note that the estimated accuracy of CASPT2 to describe spin-splittings is ∼12 kJ/mol.[12,14]

Table 2. Comparison of Several DFT Functionals and Semiempirical Methods with the CASPT2 Reference[a]

method	STDEV	MAE
B2PLYP	38.4	108.6
B3LYP	39.9	113.7
B3LYP-D3	38.4	105.2
BLYP	54.2	143.5
BP86	49.2	134.7
M06	17.8	31.8
O3LYP	25.4	83.1
OLYP	19.5	75.0
OPBE	26.9	83.8
PBE0	32.6	92.8
PM6[b]	79.7	319.7
PM6R[b]	25.2	67.5
TPSS	52.8	143.6
TPSSh	46.4	122.5

[a]Standard deviations (STDEV) and maximum absolute errors (MAE) of relative energies (in kilojoules per mole) for structures from the $Fe(SH)_4$ ferric−thiolate bond dissociation pathways. Values obtained from the relative energies (Table S2) of nine single-point calculations, corresponding to the six structures shown in Figure 2 (both quartet and sextet states were calculated for the MECP), ^{2}R and ^{2}P. [b]PM6 is the original semiempirical parametrization and PM6R is the parametrization obtained in this work (Table S1).

An analysis of the data shows that the best performing functional is the M06 hybrid meta-GGA, followed by the simpler OLYP pure-GGA functional, although with a much larger maximum error. The doublet states have the highest relative energies and give the maximum errors for all functionals except B2PLYP and M06. The OLYP functional is followed closely by OPBE and O3LYP, suggesting that Handy and Cohen's OPTX exchange functional[29] is the most appropriate to describe Fe−S bond dissociation. This exchange functional includes some nondynamic electron correlation effects (named "left−right correlation")[29] that contribute to the correct description of homolytic bond dissociation. On the other hand, Becke's one-parameter exchange functional,[40] used in BLYP and BP86, performs significantly worse. This is because it stays closer to the uniform electron gas assumption (the Dirac coefficient is not scaled)[29] and does not include such left−right nondynamic correlation effects.

Apart from the highly parametrized M06, meta-GGA functionals, such as TPSS, do not perform particularly well. Inclusion of Hartree−Fock exchange does not markedly improve the results for TPSSh in comparison to TPSS. By contrast, hybrid functionals, such as B3LYP and PBE0, do show lower errors, especially for energy splittings between different spin states. It should be noted that the pure GGA functionals not based on the OPTX exchange functional, such as BLYP, BP86, and TPSS, give a qualitatively wrong description of the spin splitting, as ^{4}R is more stable than ^{6}R (Table S2). Mixing some exact exchange with the OPTX functional as in O3LYP does not improve the spin splittings in comparison to the pure-GGA OLYP. The double-hybrid functional B2PLYP does not perform significantly better, suggesting that the inclusion of dynamic correlation effects via an MP2 contribution is not important for the description of ferric−thiolate bond dissociation. Finally, inclusion of dispersion corrections as in the B3LYP-D3 functional does not change the relative energies, in comparison to the B3LYP functional.

DOI: 10.1021/acs.jpca.5b05658
J. Phys. Chem. A 2015, 119, 10084−10090

We conclude that the hybrid M06 functional and the functionals based on Handy and Cohen's OPTX exchange give the best results for iron−sulfur bond dissociation. If computational efficiency is important, then the pure-GGA functionals OLYP and OPBE are to be preferred.

Given that we are particularly interested in the simulation of iron−sulfur clusters in complex systems, we wanted to evaluate methods that are computationally more efficient than CASPT2 and DFT. As an initial choice, we tried the recent semiempirical Hamiltonian PM6[30] that contains d-orbitals in its minimal basis-set and was parametrized for molecules containing iron. These tests, using unrestricted HF (UHF) and ROHF + CASCI calculations and the original PM6 Hamiltonian, resulted in a very poor description of ferric−thiolate bond dissociation energetics (Table 2 and Table S2, which show the ROHF + CASCI results only). This poor performance is due to an incorrect MO ordering, as the orbital formed mainly by the Fe 4s-shell was occupied and lower in energy than the MOs composed by the Fe 3d open-shell, suggesting an imbalance between the semiempirical ζ_s and ζ_d orbital coefficients. Our previous experience[58] indicates that this imbalance can be corrected by a specific reparametrization of the iron PM6 parameters. This we did successfully, leading to a parametrization that we denote PM6R (Table S1).

ROHF + CASCI calculations with the new PM6R Hamiltonian perform rather well, with deviations similar to functionals based on OPTX exchange, but with smaller maximum errors (Table 2). However, this is not a fair comparison because the CASPT2 reference energies were actually used to fit the PM6R parameters. The observed MO orbital ordering is indeed similar to that obtained for the ab initio CASSCF wave functions with, in increasing order of energy, doubly occupied ligand MOs, singly occupied MOs corresponding to the Fe 3d shell, and an unoccupied Fe 4s shell. The resulting spin densities are consequently more accurate and close to those shown in Table 1. However, it should be noted that UHF calculations with the new parameters yielded poor results. Thus, although our specifically parametrized semiempirical Hamiltonian, in conjunction with CI calculations, can describe the energetics and electronic configuration of ferric−thiolate bond dissociation rather well, the transferability and applicability of these new parameters in other circumstances needs to be further validated.

4. CONCLUSIONS

We have studied ferric−thiolate bond dissociation in the isolated model iron−sulfur tetrahedral compounds, $Fe(SH)_4^-$ and $Fe(SCH_3)_4^-$, using the multiconfigurational wave function methods, ab initio CASPT2 and semiempirical CASCI, and several DFT functionals. The reaction proceeds via a homolytic mechanism with a spin crossing between the sextet and quartet states. This two-state reactivity is often seen in transition-metal compounds,[59] and so studies of the stability, reactivity, and biosynthesis of iron−sulfur clusters in proteins need to carefully account for the different accessible spin states.

The high-level CASPT2 method was used as a reference, against which the various other electronic structure approaches were compared. We find that the M06 functional is the best for describing Fe−S bond dissociation when all possible spin states are to be considered. Our DFT comparisons are also in agreement with previous studies[14] that highlight the reliability of the OLYP and OPBE functionals for describing iron complexes. The B3LYP functional gives satisfactory results, and it should be fairly dependable for geometry optimizations.

Ferric−thiolate bond dissociation is a difficult problem to model as it involves different kinds of electron correlation effects that change unevenly as the reaction progresses. Near-degenerate nondynamic correlation is important for describing the multiplet structure of the ferric center and, consequently, the energy splittings between the various spin states. By contrast, left−right nondynamic correlation is critical for the description of homolytic bond dissociation, whereas angular correlation in the transition metal also needs to be considered appropriately, given the change in metal coordination from tetrahedral reactants to trigonal products. As a result, this reaction constitutes a tough test for electronic structure methods, in particular for the single-determinant, principally DFT, approaches tried here.

We conclude by noting that specifically parametrized semiempirical methods employing d-orbitals and CI calculations can be used to model the Fe−S dissociation reaction, but further studies are necessary to evaluate the general applicability of this approach.

■ ASSOCIATED CONTENT

Supporting Information

The Supporting Information is available free of charge on the ACS Publications website at DOI: 10.1021/acs.jpca.5b05658.

Tables containing the reoptimized PM6 iron semiempirical parameters and the relative energies calculated with all the electronic structure methods used here (PDF)

■ AUTHOR INFORMATION

Corresponding Author

*E-mail: garantes@iq.usp.br.

Notes

The authors declare no competing financial interest.

■ ACKNOWLEDGMENTS

Funding from FAPESP (12/02501-4 and 14/21900-2) and a joint FAPESP-CNRS project (23277) are gratefully acknowledged.

■ REFERENCES

(1) Beinert, H.; Holm, R. H.; Munck, E. Iron-Sulfur Clusters: Nature's Modular, Multipurpose Structures. *Science* **1997**, *277*, 653−659.

(2) Holm, R. H.; Kennepohl, P.; Solomon, E. I. Structural and Functional Aspects of Metal Sites in Biology. *Chem. Rev.* **1996**, *96*, 2239−2314.

(3) Solomon, E. I.; Gorelsky, S. I.; Dey, A. Metal-Thiolate Bonds in Bioinorganic Chemistry. *J. Comput. Chem.* **2006**, *27*, 1415−1428.

(4) Zheng, P.; Li, H. Highly Covalent Ferric-Thiolate Bonds Exhibit Surprisingly Low Mechanical Stability. *J. Am. Chem. Soc.* **2011**, *133*, 6791−6798.

(5) Arantes, G. M.; Bhattacharjee, A.; Field, M. J. Homolytic Cleavage of Fe-S Bonds in Rubredoxin Under Mechanical Stress. *Angew. Chem., Int. Ed.* **2013**, *52*, 8144−8146.

(6) Zheng, P.; Arantes, G. M.; Field, M. J.; Li, H. Force Induced Chemical Reactions on the Metal Center in a Single Metalloprotein Molecule. *Nat. Commun.* **2015**, *6*, 7569.

(7) Beinert, H. Iron-Sulfur Proteins: Ancient Structures, Still Full of Surprises. *JBIC, J. Biol. Inorg. Chem.* **2000**, *5*, 2−15.

(8) Helgaker, T.; Jørgensen, P.; Olsen, J. *Molecular Electronic-Structure Theory*, 1st ed.; Wiley: New York, 2000.

DOI: 10.1021/acs.jpca.5b05658
J. Phys. Chem. A 2015, 119, 10084−10090

(9) Roos, B. O.; Taylor, P. R.; Siegbahn, P. E. M. A Complete Active Space SCF Method (CASSCF) Using a Density Matrix Formulated Super-CI Approach. *Chem. Phys.* **1980**, *48*, 157−173.
(10) Andersson, K.; Malmqvist, P. A.; Roos, B. O. Second-Order Perturbation Theory with a Complete Active Space Self-Consistent Field Reference Function. *J. Chem. Phys.* **1992**, *96*, 1218.
(11) Pierloot, K. *Nondynamic Correlation Effects in Transition Metal Coordination Compounds*, 1st ed.; Marcel Dekker: New York, 2001; pp 123−158.
(12) Pierloot, K.; Vancoillie, S. Relative Energy of the High-($^5T_{2g}$) and Low-($^1A_{1g}$) Spin States of $[Fe(H_2O)_6]^{2+}$, $[Fe(NH_3)_6]^{2+}$, and $[Fe(bpy)_3]^2$+: CASPT2 Versus Density Functional Theory. *J. Chem. Phys.* **2006**, *125*, 124303.
(13) Arantes, G. M.; Taylor, P. R. Approximate Multiconfigurational Treatment of Spin-Coupled Metal Complexes. *J. Chem. Theory Comput.* **2010**, *6*, 1981−1989.
(14) Swart, M. Accurate Spin-State Energies for Iron Complexes. *J. Chem. Theory Comput.* **2008**, *4*, 2057−2066.
(15) Parr, R. G.; Yang, W. *Density-Functional Theory of Atoms and Molecules*, 1st ed.; Oxford University Press: Oxford, 1996.
(16) Cramer, C. J.; Truhlar, D. G. Density Functional Theory for Transition Metals and Transition Metal Chemistry. *Phys. Chem. Chem. Phys.* **2009**, *11*, 10757−10816.
(17) Reiher, M.; Salomon, O.; Hess, B. A. Reparameterization of Hybrid Functionals Based on Energy Differences of States of Different Multiplicity. *Theor. Chem. Acc.* **2001**, *107*, 48−55.
(18) Swart, M.; Groenhof, A. R.; Ehlers, A. W.; Lammertsma, K. Validation of Exchange-Correlation Functionals for Spin States of Iron Complexes. *J. Phys. Chem. A* **2004**, *108*, 5479−5483.
(19) Jensen, K. P.; Roos, B. O.; Ryde, U. Performance of Density Functionals for First Row Transition Metal Systems. *J. Chem. Phys.* **2007**, *126*, 014103.
(20) Jensen, K. P. Bioinorganic Chemistry Modeled with the TPSSh Density Functional. *Inorg. Chem.* **2008**, *47*, 10357−10365.
(21) Sorkin, A.; Iron, M. A.; Truhlar, D. G. Density Functional Theory in Transition-Metal Chemistry: Relative Energies of Low-Lying States of Iron Compounds and the Effect of Spatial Symmetry Breaking. *J. Chem. Theory Comput.* **2008**, *4*, 307−315.
(22) Niu, S.; Nichols, J. A.; Ichiye, T. Optimization of Spin-Unrestricted Density Functional Theory for Redox Properties of Rubredoxin Redox Site Analogues. *J. Chem. Theory Comput.* **2009**, *5*, 1361−1368.
(23) Bergeler, M.; Stiebritz, M. T.; Reiher, M. Structure-Property Relationships of Fe4S4 Clusters. *ChemPlusChem* **2013**, *78*, 1082−1098.
(24) Bruska, M. K.; Stiebritz, M. T.; Reiher, M. Analysis of Differences in Oxygen Sensitivity of Fe-S Clusters. *Dalton Trans.* **2013**, *42*, 8729−8735.
(25) Ye, S.; Neese, F. Accurate Modeling of Spin-State Energetics in Spin-Crossover Systems with Modern Density Functional Theory. *Inorg. Chem.* **2010**, *49*, 772−774.
(26) Isley, W. C., III; Zarra, S.; Carlson, R. K.; Bilbeisi, R. A.; Ronson, T. K.; Nitschke, J. R.; Gagliardi, L.; Cramer, C. J. Predicting Paramagnetic ^{1}H NMR Chemical Shifts and State-Energy Separations in Spin-Crossover Host-Guest Systems. *Phys. Chem. Chem. Phys.* **2014**, *16*, 10620−10628.
(27) Ferre, N.; Guihery, N.; Malrieu, J.-P. Spin Decontamination of Broken-Symmetry Density Functional Theory Calculations: Deeper Insight and New Formulations. *Phys. Chem. Chem. Phys.* **2015**, *17*, 14375−14382.
(28) Tao, J. M.; Perdew, J. P.; Staroverov, V. N.; Scuseria, G. E. Climbing the Density Functional Ladder: Nonempirical Meta-Generalized Gradient Approximation Designed for Molecules and Solids. *Phys. Rev. Lett.* **2003**, *91*, 146401.
(29) Handy, N. C.; Cohen, A. J. Left-Right Correlation Energy. *Mol. Phys.* **2001**, *99*, 403−412.
(30) Stewart, J. J. P. Optimization of Parameters for Semiempirical Methods V: Modification of NDDO Approximations and Application to 70 Elements. *J. Mol. Model.* **2007**, *13*, 1173−1213.
(31) Becke, A. D. Density Functional Thermochemistry. III. The Role of Exact Exchange. *J. Chem. Phys.* **1993**, *98*, 5648.
(32) Lee, C.; Yang, W.; Parr, R. Development of the Colle-Salvetti Correlation-Energy Formula into a Functional of the Electron Density. *Phys. Rev. B: Condens. Matter Mater. Phys.* **1988**, *37*, 785−789.
(33) Ditchfield, R.; Hehre, W.; Pople, J. A. Self-Consistent Molecular-Orbital Methods. IX. An Extended Gaussian-Type Basis for Molecular-Orbital Studies of Organic Molecules. *J. Chem. Phys.* **1971**, *54*, 724−728.
(34) Schäfer, A.; Horn, H.; Ahlrichs, R. Fully Optimized Contracted Gaussian Basis Sets for Atoms Li to K. *J. Chem. Phys.* **1992**, *97*, 2571−2577.
(35) Frisch, M. J.; Trucks, G. W.; Schlegel, H. B.; Scuseria, G. E.; Robb, M. A.; Cheeseman, J. R.; Scalmani, G.; Barone, V.; Mennucci, B.; Petersson, G. A. et al. *Gaussian 09*, revision A.1; Gaussian, Inc.: Wallingford, CT, 2009.
(36) Field, M. J. The pDynamo Program for Molecular Simulations using Hybrid Quantum Chemical and Molecular Mechanical Potentials. *J. Chem. Theory Comput.* **2008**, *4*, 1151−1161.
(37) Neese, F. The ORCA Program System. *Wiley Interdiscip. Rev.: Comput. Mol. Sci.* **2012**, *2*, 73−78.
(38) Perdew, J. P.; Burke, K.; Ernzerhof, M. Generalized Gradient Approximation Made Simple. *Phys. Rev. Lett.* **1996**, *77*, 3865−3868.
(39) Adamo, C.; Barone, V. Toward Reliable Density Functional Methods Without Adjustable Parameters: The PBE0 model. *J. Chem. Phys.* **1999**, *110*, 6158−6170.
(40) Becke, A. D. Density-Functional Exchange-Energy Approximation with Correct Asymptotic Behavior. *Phys. Rev. A: At., Mol., Opt. Phys.* **1988**, *38*, 3098−3100.
(41) Perdew, J. P. Density-Functional Approximation for the Correlation Energy of the Inhomogeneous Electron Gas. *Phys. Rev. B: Condens. Matter Mater. Phys.* **1986**, *33*, 8822−8824.
(42) Zhao, Y.; Truhlar, D. G. The M06 Suite of Density Functionals for Main Group Thermochemistry, Thermochemical Kinetics, Noncovalent Interactions, Excited States, and Transition Elements: Two New Functionals and Systematic Testing of Four M06-Class Functionals and 12 Other Functionals. *Theor. Chem. Acc.* **2008**, *120*, 215−241.
(43) Schwabe, T.; Grimme, S. Double-Hybrid Density Functionals with Long-Range Dispersion Corrections: Higher Accuracy and Extended Applicability. *Phys. Chem. Chem. Phys.* **2007**, *9*, 3397.
(44) Weigend, F.; Ahlrichs, R. Balanced Basis Sets of Split Valence, Triple Zeta Valence and Quadruple Zeta Valence Quality for H to Rn: Design and Assessment of Accuracy. *Phys. Chem. Chem. Phys.* **2005**, *7*, 3297−3305.
(45) Weigend, F. Accurate Coulomb-Fitting Basis Sets for H to Rn. *Phys. Chem. Chem. Phys.* **2006**, *8*, 1057−1065.
(46) Aquilante, F.; De Vico, L.; Ferré, N.; Ghigo, G.; Malmqvist, P.-A.; Neogrády, P.; Pedersen, T. B.; Pitonak, M.; Reiher, M.; Roos, B. O.; et al. MOLCAS 7: The Next Generation. *J. Comput. Chem.* **2010**, *31*, 224−247.
(47) Roos, B. O.; Lindh, R.; Malmqvist, P.-A.; Veryazov, V.; Widmark, P.-O. New Relativistic ANO Basis Sets for Transition Metal Atoms. *J. Phys. Chem. A* **2005**, *109*, 6575−6579.
(48) Roos, B. O.; Andersson, K.; Fülscher, M. P.; Serrano-Andrés, L.; Pierloot, K.; Merchan, M.; Molina, V. Applications of Level Shift Corrected Perturbation Theory in Electronic Spectroscopy. *J. Mol. Struct.: THEOCHEM* **1996**, *388*, 257−276.
(49) Granucci, G.; Toniolo, A. Molecular Gradients for Semiempirical CI Wavefunctions with Floating Occupation Molecular Orbitals. *Chem. Phys. Lett.* **2000**, *325*, 79−85.
(50) Slavícek, P.; Martínez, T. J. Ab Initio Floating Occupation Molecular Orbital-Complete Active Space Configuration Interaction: An Efficient Approximation to CASSCF. *J. Chem. Phys.* **2010**, *132*, 234102.
(51) Ralchenko, Y.; Kramida, A. E.; Reader, J. NIST ASD Team, NIST Atomic Spectra Database (version 3.1.5). National Institute of Standards and Technology, Gaithersburg, MD, http://physics.nist.gov/asd3 (accessed March 7, 2012).

DOI: 10.1021/acs.jpca.5b05658
J. Phys. Chem. A 2015, 119, 10084−10090

(52) Butcher, K. D.; Didziulis, S. V.; Briat, B.; Solomon, E. I. Variable Photon Energy Photoelectron Spectroscopy on $FeCl_4^-$: An Unusual Electronic Structure for High-Spin d5 Complexes. *J. Am. Chem. Soc.* **1990**, *112*, 2231−2242.
(53) Noodleman, L.; Norman, J. G., Jr; Osborne, J. H.; Aizman, A.; Case, D. A. Models for Ferredoxins: Electronic Structures of Iron-Sulfur Clusters with One, Two, and Four Iron Atoms. *J. Am. Chem. Soc.* **1985**, *107*, 3418−3426.
(54) Noodleman, L.; Peng, C.; Case, D.; Mouesca, J.-M. Orbital Interactions, Electron Delocalization and Spin Coupling in Iron-Sulfur Clusters. *Coord. Chem. Rev.* **1995**, *144*, 199−244.
(55) Noodleman, L.; Han, W.-G. Structure, Redox, pKa, Spin. A Golden Tetrad for Understanding Metalloenzyme Energetics and Reaction Pathways. *JBIC, J. Biol. Inorg. Chem.* **2006**, *11*, 674−694.
(56) Solomon, E. I.; Randall, D. W.; Glaser, T. Electronic Structures of Active Sites in Electron Transfer Metalloproteins: Contributions to Reactivity. *Coord. Chem. Rev.* **2000**, *200*, 595−632.
(57) Niu, S.; Wang, X.-B.; Yang, X.; Wang, L.-S.; Ichiye, T. Mechanistic Insight into the Symmetric Fission of [4Fe-4S] Analogue Complexes and Implications for Cluster Conversions in Iron-Sulfur Proteins. *J. Phys. Chem. A* **2004**, *108*, 6750−6757.
(58) Arantes, G. M.; Loos, M. Specific Parametrisation of a Hybrid Potential to Simulate Reactions in Phosphatases. *Phys. Chem. Chem. Phys.* **2006**, *8*, 347−353.
(59) Schroder, D.; Shaik, S.; Schwarz, H. Two-State Reactivity as a New Concept in Organometallic Chemistry. *Acc. Chem. Res.* **2000**, *33*, 139−145.

DOI: 10.1021/acs.jpca.5b05658
J. Phys. Chem. A 2015, 119, 10084−10090